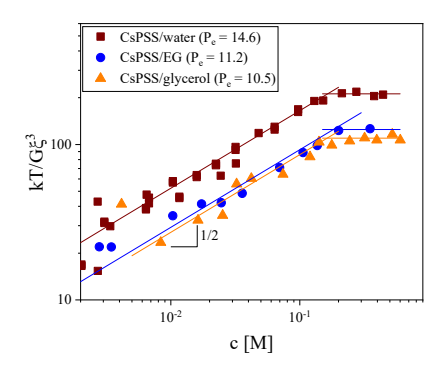
# Rheology of entangled polyelectrolyte solutions

Aijie Han and Ralph H. Colby\*

Materials Science and Engineering and Materials Research Institute,

Pennsylvania State University, University Park, PA 16802

## For ToC use only:



#### **Abstract**

Polyelectrolyte solution dynamics have been carefully studied experimentally and theoretically for unentangled solutions and thought to be reasonably well understood. While theoretical models have been proposed for entangled polyelectrolyte solutions, there have been limited experimental data published to justify any understanding of entangled polyelectrolyte solution rheology. Herein, we study entangled nearly monodisperse carefully dialyzed cesium polystyrene sulfonate (CsPSS,  $M_n = 2.83 \times 10^6$  g/mol) solutions without salt in water, anhydrous ethylene glycol ( $T_g = -95$  °C) and anhydrous glycerol ( $T_g = -80$  °C) using rotational rheometry and X-ray scattering to determine the correlation length. For the glycerol solutions, time-temperature superposition was found to work between 25 °C and -5 °C, yielding linear viscoelastic (LVE) response of polyelectrolyte solutions over a wide frequency range. At concentrations where scaling predictions expect entanglements, the LVE response appears unentangled (no rubbery plateau), suggesting an underestimation of the entanglement concentration  $c_e$ . At higher concentrations in entangled solutions, the rubbery plateau width, measured as the ratio of the two crossing points of storage and loss moduli ( $\tau_{rep}/\tau_e$ )

in glycerol scales as c<sup>4</sup>, suggesting that polyelectrolyte solutions behave like solutions of neutral polymers in the entangled concentration regime. Four methods for evaluating entanglement concentration are compared and their relative orderings are similar to those of neutral polymer solutions.

#### 1. Introduction

Polyelectrolytes are widely used in solutions as flow modifiers for coatings and stabilizers in colloidal suspensions, due to the electrostatic interactions between ionized groups while dissolved in water. The dynamics of unentangled polyelectrolyte solutions with no added salt are well understood<sup>1</sup> using the scaling model.<sup>2-4</sup> However, entangled solution dynamics remains an elusive topic. Some research effort has been devoted to the theoretical understanding of entangled polyelectrolyte solutions, but there are limited experimental data to test any theories. Also, many published experimental results strongly disagree with scaling predictions.<sup>1,3,5,6</sup> It is important to understand the dynamics of entangled polyelectrolyte solutions for both industrial use and the development of fundamental polymer science.

Some static properties such as correlation length and terminal modulus, and dynamic properties such as specific viscosity and terminal relaxation time have been studied exhaustively and some universal laws have been established for simple highly charged flexible synthetic polyelectrolyte systems.<sup>1, 5, 7</sup> Dou and Colby<sup>8, 9</sup> have studied partially quaternized poly(2-vinyl pyridine) with chloride counterions at various charge fraction in ethylene glycol (EG) solutions and no residual salt effects are reported. In the semidilute unentangled regime, the well-known Fuoss law<sup>10-12</sup> is observed for solution viscosity; the concentration dependence of relaxation time ( $\tau$ ) also agrees with the scaling prediction.<sup>8</sup> In the entangled regime, there are two crossover points in the entangled regime from viscosity data: entanglement concentration (c<sub>e</sub>) and overlap concentration of electrostatic blobs (c<sub>D</sub>). Above c<sub>D</sub>, polyelectrolyte chain conformations are unperturbed by electrostatic interactions and solutions behave like neutral polymers in good solvents which was shown in the power law exponent of the concentration dependence of specific viscosity. Furthermore, at high concentrations above c<sub>D</sub>, the polyelectrolyte specific viscosity merges with that of neutral poly(2vinyl pyridine) in EG. This is expected, since EG is a good solvent for neutral poly(2-vinyl pyridine), making the electrostatic blobs for partially quaternized poly(2-vinyl pyridine) in EG quite large. Additionally, the relaxation time is shown to be independent of concentration between ce and cD, and then becomes an increasing function of concentration above c<sub>D</sub> which has also been seen in simulation studies.<sup>13</sup>

The increase in relaxation time is not expected for polyelectrolytes with no salt and is attributed to a crossover to neutral polymer solutions. Terminal modulus G can be calculated from the ratio of viscosity and relaxation time at various concentrations. Below  $c_e$ , G increases linearly with c and is quantitatively kT per chain; above  $c_e$ , G increases with a stronger concentration dependence ( $G \sim c^{3/2}$ ) due to entanglement effects. However, from the concentration dependence of terminal modulus,  $c_e$  and  $c_D$  cannot be discerned anymore: the crossover between  $G \sim c$  and  $G \sim c^{3/2}$  does not agree well with either  $c_e$  or  $c_D$ .

The fact that the crossover point from the concentration dependence of terminal modulus occurs between  $c_e$  and  $c^*$  raised the question whether solutions between  $c_e$  and  $c_D$  are truly entangled. The easiest way to study the entanglement dynamics is through linear viscoelastic (LVE) response of these solutions. However, with commercially available rheometers, the LVE response of aqueous polyelectrolyte solutions is limited to the terminal regime for currently available chain lengths. The storage and loss moduli crossover at low frequency ( $\tau_{rep}$ ) can sometimes be observed for high molecular weight sodium carboxymethyl cellulose (NaCMC). However, NaCMC aqueous solutions might have association effects between chain backbones through strong hydrogen bonding which adds more complexities to decouple entanglement and interchain association. Acoustic rheometers can be used to study the linear viscoelastic response as these extend the measurable frequency range up to  $10^4$  Hz. However, a better understanding of this type of rheometer is required to interpret the data.

In this article, we study the entangled solution dynamics of polyelectrolyte solutions using more viscous solvents, in order to slow down the dynamics (all relaxation times are proportional to solvent viscosity). Rheological measurements under oscillatory shear at various temperatures have been performed in order to create master curves. Nearly monodisperse cesium polystyrene sulfonate (CsPSS) represents a polyelectrolyte model system as it has the same backbone as NaPSS, and the Cs<sup>+</sup> counterion facilitates inhouse X-ray scattering. We show that salt-free solutions of CsPSS in glycerol exhibit identical entanglement dynamics as neutral polymer solutions.

# **Background Theory**

Entangled neutral polymer solutions and melts. Many models have been proposed to explain the dynamics of entangled polymers. Among them, the Doi-Edwards reptation model<sup>18-20</sup> is well recognized to describe the entangled dynamics of linear flexible neutral polymer solutions. Polymer chain relaxation is modelled as reptation; a Rouse motion of each chain along a tube constructed by neighboring chains (entanglements).<sup>21, 22</sup> The tube diameter a is defined as the average end-to-end distance of one entanglement strand that is a random walk of  $N_e$  Kuhn monomers.<sup>23</sup>

$$a \approx bN_e^{1/2} \tag{1}$$

Here b is the Kuhn length and  $N_e$  is the number of Kuhn monomers in one entanglement strand which has molecular weight  $M_e = N_e M_0$  ( $M_0$  is the molecular weight of a Kuhn monomer) defined by the measurable plateau modulus  $G_e$  expressed as kT per entanglement strand.<sup>24</sup>

$$G_e = \frac{\rho RT}{M_o} \sim c^{2.3}$$
 for neutral polymers in any solvent (2)

Here  $\rho$  is the mass density and R is the gas constant. Graessley and Edwards<sup>25</sup> studied the viscoelastic response of entangled solutions of neutral linear polymer chains such as polystyrene and polybutadiene. They discovered the plateau modulus  $G_e$  increases with concentration as a power law  $c^{\beta}$  where  $\beta$  ranges from 2.1 to 2.3 for neutral polymer solutions.<sup>25</sup> The range of exponents comes from ignoring the melt value of the plateau modulus;<sup>6</sup> when that value is included, the exponent for neutral polymers in both good and  $\theta$ -solvents is universally 2.3.<sup>23</sup>

Regarding the dynamics, different length scales are considered to account for the relaxation of chains. Inside one entanglement strand, the topological constraints are not important, so the  $N_e/g$  correlation blobs in an entanglement strand relax as a Rouse chain (g is the number of Kuhn monomers per correlation blob) leading to a scaling prediction of the Rouse time of an entanglement strand for neutral polymer solutions that depends on solvent quality.<sup>23</sup>

$$\tau_e \cong \tau_{\xi} \left(\frac{N_e}{g}\right)^2 \sim \begin{cases} c^{-3\nu/(3\nu-1)} & \text{in athermal solvent} \\ c^{-5/3} & \text{in } \theta\text{-solvent} \end{cases}$$
 (3)

Here  $\tau_{\xi}$  is the relaxation time within one correlation blob of g monomers, estimated by the Zimm model and v is the Flory exponent (coil size scales as N<sup>v</sup> in dilute solution). The reptation time  $\tau_{rep}$  is the time it takes for the chain of N Kuhn monomers to diffuse out of the tube.

$$\tau_{rep} \cong \tau_e \left(\frac{N}{N_e}\right)^3 \sim \begin{cases} c^{3(1-\nu)/(3\nu-1)} & \text{in athermal solvent} \\ c^{7/3} & \text{in } \theta\text{-solvent} \end{cases}$$
 (4)

For athermal and good solvents,  $v \approx 0.588$  leads to  $\tau_e \sim c^{-2.3}$  and  $\tau_{rep} \sim c^{1.6}$ . Thus, for linear flexible neutral polymer solutions, the ratio of  $\tau_{rep}$  to  $\tau_e$ , a measure of the width of the rubbery plateau, follows a power law dependence of concentration  $c^4$ , independent of solvent quality.

$$\frac{\tau_{rep}}{\tau_e} \cong \left(\frac{N}{N_e}\right)^3 \sim c^4 \quad \text{for neutral polymers in any solvent}$$
 (5)

The concentration dependences of  $\tau_{rep}$  and  $\tau_e$  have been tested experimentally for neutral polymer solutions. The LVE response shows two frequencies where storage and loss moduli cross; the low frequency crossing is taken to be at angular frequency  $1/\tau_{rep}$  and the high frequency crossing is taken to be at angular frequency  $1/\tau_e$ . The glass transition temperature of the solution can of course change with concentration, affecting both  $\tau_{rep}$  and  $\tau_e$  in the same way and not affecting their ratio. Baumgärtel and Willenbacher studied oscillatory shear rheology of concentrated polystyrene/ethylbenzene solutions at temperatures from 80 °C to -50 °C, depending on the glass transition temperature of different polymer fractions.<sup>26</sup> Master curves generated for each concentration show a clear rubbery plateau. The plateau modulus  $G_e$  scales as  $c^{2.3}$  as expected.<sup>25, 26</sup> From their master curves, we find below that the plateau width  $\tau_{rep}/\tau_e$  scales as a power law of  $c^4$ , as expected for neutral polymers in any solvent (eq. 5).

Unentangled polyelectrolyte solutions. In dilute salt-free polyelectrolyte solutions, the chains adopt an extended conformation due to the electrostatic repulsion between charged groups. The extended conformation can be quantified by the chain contraction factor B, which is defined as the ratio of chain contour (bN) length and its extended chain size (L) in dilute salt-free solutions  $^3$  B  $\equiv$  bN/L. Ideally, b is the Kuhn length and N is the number of Kuhn monomers in the flexible polyelectrolyte chain. However, the Kuhn length of polyelectrolytes has never been measured so here we take b = 0.25 nm, the length of the chemical repeat unit and then N is the degree of polymerization. B depends on solvent quality and the extent of counterion condensation. The Bjerrum length is the length scale where the Coulomb energy of two charges is the same magnitude as the thermal energy kT.

$$l_B = \frac{e^2}{\varepsilon kT} \tag{6}$$

Here e is the elementary charge and  $\varepsilon$  is the dielectric constant of the solvent. Bjerrum length is an important length scale according to Manning's counterion condensation theory<sup>27</sup>, as there is only one effective charge per l<sub>B</sub>. Due to the highly extended conformation of polyelectrolyte chains in salt-free solutions, c\* decreases rapidly with the degree of polymerization.<sup>3</sup>

$$c^* \approx \frac{N}{L^3} \approx \frac{B^3}{b^3 N^2} \tag{7}$$

Boris and Colby<sup>1</sup> showed that  $c^*$  scales as  $N^{-2}$  for salt-free sodium polystyrene sulfonate (NaPSS) aqueous solutions, in agreement with the scaling prediction (eq. 7). The correlation length  $\xi$  becomes an important length scale above  $c^*$ , as  $\xi$  is the average distance between neighboring chains. Electrostatic interactions are predicted to be screened on length scales above the correlation length ( $\xi$ ) in semidilute solutions,<sup>3</sup> making the chains random walks of correlation blobs, inside of which the chains are strongly extended by electrostatic repulsion with no salt present. In semidilute unentangled solutions, the Rouse model can be applied to describe the terminal relaxation. The scaling theory proposed by Dobrynin et al<sup>3</sup> utilizes the Rouse model and derived the concentration dependence of relaxation time ( $\tau$ ) which is predicted to decrease with concentration as  $c^{-1/2}$  for salt-free semidilute unentangled polyelectrolyte solutions, and since the

terminal modulus G = ckT/N (kT per chain for any unentangled solution), the concentration dependence of the polymer's contribution to solution viscosity ( $\eta$ -  $\eta_s$ ) scales as  $c^{1/2}$ , the well-known Fuoss law. <sup>10-12</sup> Both  $\tau$  and  $\eta$  can be easily measured from steady shear rheology and their concentration dependences have been confirmed experimentally with both polycations and polyanions. <sup>1,5,8,28</sup>

Entangled Polyelectrolyte Solutions. The crossover from the unentangled to the entangled regime marks the entanglement concentration c<sub>e</sub>. At c<sub>e</sub>, chains strongly overlap, and the motion of chains are topologically constrained by the presence of neighboring chains, also known as entanglement effects, where chains are not able to pass through each other.<sup>3, 14, 23, 29</sup> The entanglement concentration of salt-free polyelectrolyte solutions is predicted to have the same N dependence as c\*.<sup>3</sup>

$$c_e = c^* P_e^4 \approx \frac{B^3 P_e^4}{b^3 N^2} \tag{8}$$

 $P_{\rm e}$  is an overlap parameter for entanglement, the number of different chains inside an entanglement volume  $(a^3)$ 

$$P_e \approx \frac{a^3}{V_e} \approx \frac{a^3}{a^2 \xi} = \frac{a}{\xi} = \sqrt{\frac{kT}{G_e \xi^3}}$$
 (9)

where  $V_e \approx \xi^3 N_e/g \approx a^2 \xi$  is the occupied volume of an entanglement strand.<sup>30</sup> The reptation model is applied to describe the dynamics of entangled polyelectrolyte solutions. In the entangled regime, the plateau modulus, specific viscosity ( $\eta_{sp}$ ), longest relaxation time  $\tau_{rep}$  and Rouse time of an entanglement strand  $\tau_e$  are predicted to be <sup>3,6</sup>

$$G_e = \frac{ckT}{N_e} \sim N^0 c^{3/2} \tag{10}$$

$$\eta_{sp} \approx G_e \tau_{rep} \sim N^3 c^{3/2} \tag{11}$$

$$\tau_{rep} \approx \tau_{\xi} (\frac{N_e}{g})^2 (\frac{N}{N_e})^3 \sim N^3 c^0 \tag{12}$$

$$\tau_e \approx \tau_\xi (\frac{N_e}{g})^2 \sim N^0 c^{-3/2}$$
(13)

for salt-free polyelectrolyte solutions. Thus, the crossover of  $\eta_{sp} \sim c^{1/2}$  and  $\eta_{sp} \sim c^{3/2}$  is commonly used as the method to determine  $c_e$ , easily detected as the concentration exponent triples. It is important to note that the relaxation time in the entangled regime is predicted to be concentration independent (eq. 12) and the width of the rubbery plateau is predicted to be  $\frac{\tau_{rep}}{\tau_e} \sim N^3 c^{3/2}$  for salt-free polyelectrolyte solutions, with a much weaker concentration dependence than for neutral polymer solutions (eq. 5).

However, experimental results of salt-free polyelectrolyte solutions always show a weaker dependence of entanglement concentration on chain length, as demonstrated in fig. 1. For NaPSS aqueous solutions,  $c_e$  data are obtained from both viscosity data and diffusion measurements of Oostwal.<sup>1, 31, 32</sup> We have also added  $c_e$  of polystyrene sulfonate with cesium counterions (CsPSS) in aqueous solutions as there is little difference in  $c_e$  using these two different counterions. Overall, for polystyrene sulfonate solutions,  $c_e$  follows a power law of N<sup>-0.77</sup>, expected for neutral polymers in any solvent.<sup>21</sup> The same N dependence of  $c_e$  is found for NaCMC where  $c_e$  is also obtained from viscosity data.<sup>14, 15, 28, 33, 34</sup> Both datasets disagree with the scaling theory prediction for polyelectrolytes with no salt present (eq. 8), while the exponent of the concentration dependence of viscosity matches perfectly with the scaling theory. Thus, it is possible that the widely used crossover method to obtain  $c_e$  by detecting the concentration where  $\eta_{sp} \sim c^{1/2}$  transitions to  $\eta_{sp} \sim c^{3/2}$  might underestimate  $c_e$ . Also, there are no experimental results showing the LVE response of entangled polyelectrolyte solutions, which is crucial to prove the presence of entanglement effects. Whether entanglement exists in polyelectrolyte solutions is an important topic. Without a comprehensive understanding of what an entanglement is, it is hard to conclude the effects of electrostatic interaction on topological constraints.

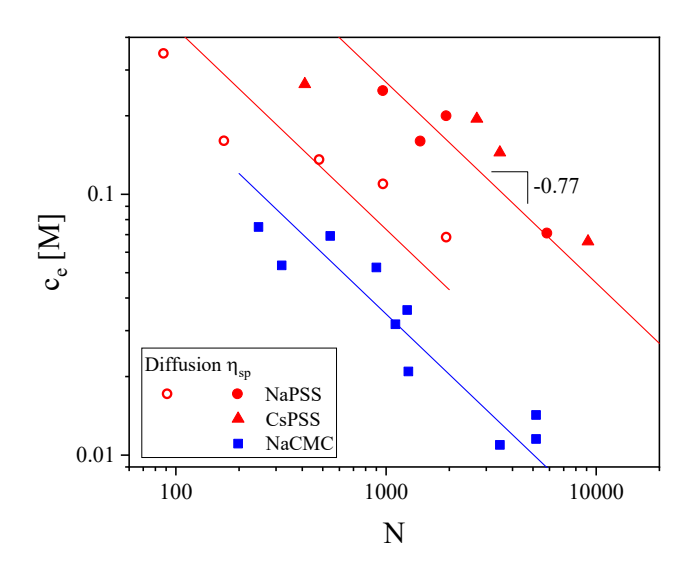


Figure 1. Entanglement concentration (c<sub>e</sub>) from the specific viscosity as a function of degree of polymerization (N) for salt-free polyelectrolyte solutions in water. Filled red circles are NaPSS aqueous solutions taken from specific viscosity<sup>1</sup> and open circles are obtained from diffusion data<sup>32</sup>. Red triangles are cesium polystyrene sulfonate (CsPSS) aqueous solutions from this work. Filled blue squares are sodium carboxymethyl cellulose aqueous solutions.<sup>14</sup> Solid lines are power law fits with exponent of -0.77, expected for neutral polymer solutions.

With the questions raised above, the dynamics of entangled polyelectrolyte solutions are still an open question due to (1) the paucity of experimental data and (2) at least some results contradicting theoretical predictions.<sup>6, 14</sup>

In this paper, we report linear viscoelastic response over a wide range of frequency for entangled polyelectrolyte solutions to compare with entangled neutral polymer solutions. Both static and dynamic properties are analyzed to have a better understanding regarding whether the reptation motion in solution of polyelectrolyte chains differs much from that of neutral polymer chains.

### 2. Experimental section

**2.1 Materials.** Narrow molecular weight distribution linear sodium polystyrene sulfonate standard (NaPSS) was purchased from Scientific Polymer Products (Webster, NY; catalog No. 923). Light scattering and gel

permeation chromatography indicate  $M_n$ = 1.89 ×10<sup>6</sup> g/mol,  $M_w$ = 2.24 ×10<sup>6</sup> g/mol,  $M_w$ / $M_n$ = 1.2, as reported by the manufacturer. The degree of sulfonation is 97% through titration. NaPSS was ion-exchanged from Na<sup>+</sup> counterion to Cs<sup>+</sup> counterion by adding 15 times excess cesium chloride salt (CsCl) in aqueous NaPSS solutions, resulting in 93% Cs<sup>+</sup> and 7% Na<sup>+</sup> counterions after ion-exchange. Exhaustive dialysis against deionized water was performed to remove the excess salt, flushing ~20 liters of water through the dialysis cell with a 30K molecular weight cutoff cellulose membrane. The dialysis is terminated after the conductivity of dialyzate is below 2  $\mu$ S/cm.

Three solvents are used to dissolve CsPSS, as shown in Table 1. CsPSS readily dissolves in deionized water (Milli-Q) and ethylene glycol (EG from Sigma-Aldrich, 99.8%, anhydrous). All measurements were performed within one week after the samples were fully dissolved. The viscosity of glycerol (Sigma-Aldrich, grade ACS reagent ≥ 99.5%, anhydrous) is much higher than water and EG (See Table 1) resulting in a much longer time (roughly a month) for CsPSS to be fully dissolved. No stirring or agitation was applied to the solution. Since EG and glycerol tend to absorb moisture from the atmosphere, those solutions were prepared in a glovebox under argon with less than 2 ppm water.

Table 1. Physical properties of solvents and experimental quantities of CsPSS solutions at 25 °C

	Viscosity <sup>a</sup>	ε	l <sub>B</sub> [nm]	$\mathrm{B}^{\mathrm{b}}$	Melting temperature	Vanor programa [Da] c	
	[mPa.s]				$(T_m)$ [°C]	Vapor pressure [Pa] <sup>c</sup>	
Water	0.89	81	0.71	1.7	0	3170	
EG	16.1	37	1.55	2.4	-13	12.3	
Glycerol	1044	42	1.37	2.3	0 <sup>d</sup>	0.0218	

<sup>&</sup>lt;sup>a</sup> Solvent viscosity values are measured using the RFS-III rheometer at 25 °C with the concentric cylinder geometry.

<sup>&</sup>lt;sup>b</sup> The values of B are calculated assuming b = 0.25 nm which is the length of one chemical repeat unit.

<sup>&</sup>lt;sup>c</sup> Data taken from ref. 35, 36.

<sup>&</sup>lt;sup>d</sup> Glycerol is a glass-former which does not easily crystallize but becomes a supercooled liquid below its melting temperature. <sup>37</sup>

**2.2 Rheology.** The shear rate dependence of viscosity of aqueous solutions was measured with a strain controlled Rheometrics Fluids Spectrometer (RFS-III) using the concentric cylinder geometry (13 mm bob length, 16.5 mm bob diameter, 17 mm cup diameter). The RFS-III rheometer with Couette geometry is our best option (compared with the two discussed below) for all aqueous solutions because there is no flow instability of the edge and the torque sensitivity of the force rebalance transducer is as low as 0.002 gm cm. The temperature was controlled by an external Julabo circulating water bath to maintain all measurements at 25 °C.

Solutions in EG and glycerol are much more viscous and very hard to load in a concentric cylinder geometry for high concentration solutions. For solution viscosity higher than 20 Pa's, a Rheometrics ARES-LS rheometer with a convection oven was used with stainless-steel cone and plate geometry having 25 mm diameter and 0.04 rad cone angle under N<sub>2</sub> flow for solutions in glycerol. A TA Instruments dynamic hybrid rheometer (DHR3) was used for solution viscosity lower than 20 Pa's due to its superior sensitivity. A stainless-steel cone and plate geometry with 60 mm diameter and 0.0178 rad cone angle was used with temperature controlled by a Peltier system that comprises the bottom plate. Both steady shear and oscillatory shear experiments were carried out. Master curves were constructed by performing oscillatory shear experiments at different temperatures to obtain the linear viscoelastic response in a wide range of frequency.

2.3 Small-angle X-ray scattering (SAXS). Transmission SAXS experiments were performed using a Xenocs Xeuss 2.0 SAXS/WAXS system with Cu radiation source ( $\lambda$ =0.154 nm) at Penn State's Materials Characterization Lab. Solution samples were loaded in a stainless-steel liquid cell sealed by two Kapton films with 1.2 mm pathlength. The typical flux of  $10^7$  photons/(cm<sup>2</sup>s) requires 1-hour exposure time for good data quality. The scattered X-ray signals were collected with a Pilatus Hybrid CMOS 2-dimensional SAXS detector at room temperature with sample to detector distance 2520 mm.

For CsPSS/glycerol solutions, the transmission SAXS experiments were carried out at the Advanced Light Source (ALS), Lawrence Berkeley National Laboratory. The incident X-ray energy was 10 keV. Samples were loaded into 1 mm diameter glass capillaries with 60 seconds exposure time due to much higher incident flux (typically 10<sup>13</sup> photons/(cm<sup>2</sup>s)) resulting in I(q) data with significantly less noise. The sample to detector distance was 3600 mm to cover a q range of 0.025 to 3.5 nm<sup>-1</sup>.

#### 3. Results and discussion

Correlation length of CsPSS solutions. Fig. 2 shows the SAXS profiles of CsPSS in three solvents: water, EG and glycerol. The correlation peaks can be clearly observed in the semidilute concentration range from 0.006 M to 0.16 M. At higher concentrations,  $\text{Cs}^+$  absorbs a substantial amount of the incident X-ray, which flattens the characteristic peak under the same exposure time (see the c = 0.3699 M CsPSS/water data at the bottom of fig. 2A). At concentrations below 0.006 M, the correlation peak is hidden under the mysterious low q upturn.

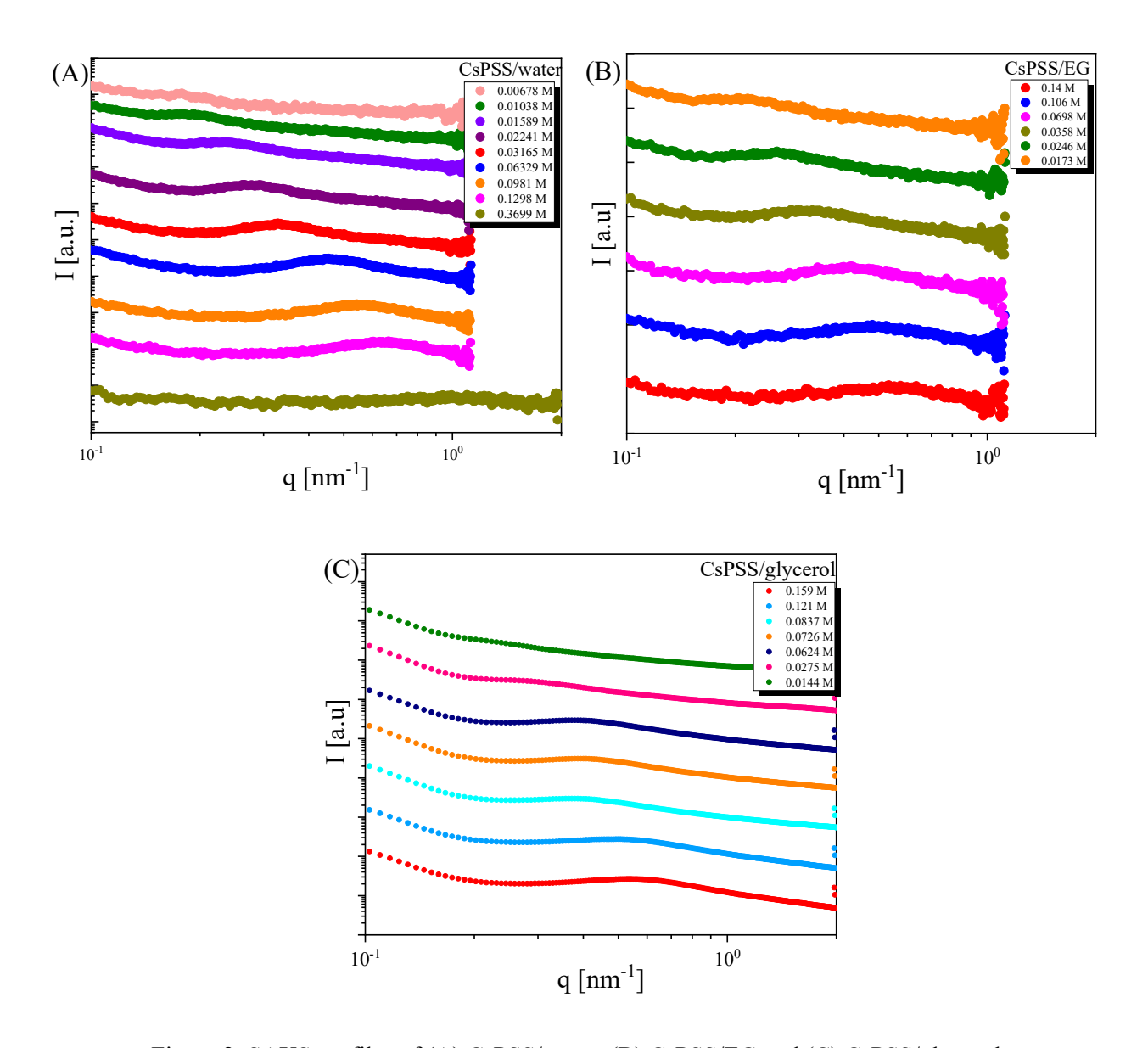


Figure 2. SAXS profiles of (A) CsPSS/water, (B) CsPSS/EG and (C) CsPSS/glycerol.

The peak position  $q_{max}$  is used to calculate the correlation length as  $\xi = 2\pi/q_{max}$ . As shown in fig. 3, the correlation length as a function of concentration follows a power law with the predicted exponent -1/2 in each of the three solvents. This concentration dependence of correlation length is expected for semidilute polyelectrolyte solutions.<sup>3,7,8</sup> The dielectric constant of each solvent is the main reason for different power

law fits, as the correlation length is related to the chain contraction factor B, as predicted by de Gennes et al.<sup>38</sup>

$$\xi = \sqrt{\frac{B}{cb}} \tag{14}$$

The chain contraction factor B is the ratio of fully extended size bN and actual dilute size. B varies with both Bjerrum length and solvent quality. Taking b as the length of one chemical repeat unit (0.25 nm), the concentration c is then the number density of repeat units and the values of B in three different solvents, calculated from the measured correlation length  $\xi = 2\pi/q_{max}$ , are listed in Table 1.

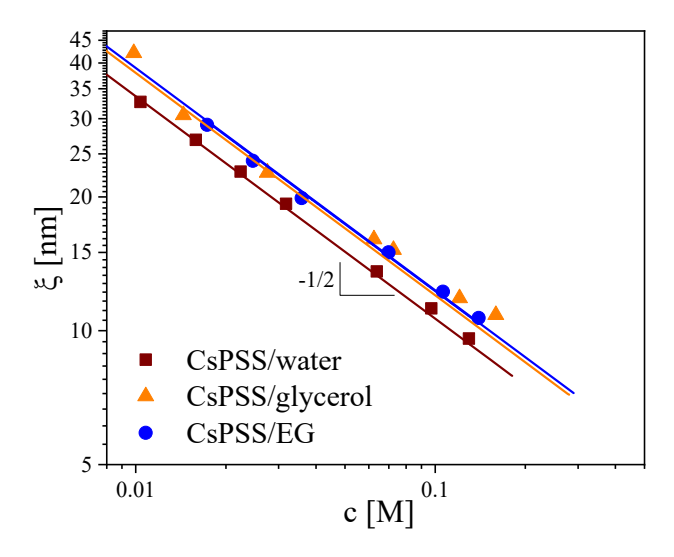


Figure 3. Correlation length  $\xi = 2\pi/q_{max}$  as a function of the solution concentration with the unit of moles of monomers per liter of solution, for three different solvents. Solid lines are fits to eq. 14, requiring the expected power law exponent of -1/2.

CsPSS/water solutions. For each concentration of CsPSS/water solution, the shear rate dependence of viscosity is plotted, as shown in fig. 4(A). The flow curves were fitted to the Carreau model to determine the zero-shear viscosity ( $\eta_0$ ) and relaxation time ( $\tau$ ) of each concentration:

$$\eta(\dot{\gamma}) = \eta_0 [1 + (\tau \dot{\gamma})^2]^{(n-1)/2}$$
 (15)

where  $\dot{\gamma}$  is the shear rate and n is the power law index of the shear thinning regime.

The Newtonian region of flow curves gives the zero-shear viscosity at each concentration, which is used as a fixed parameter for the Carreau model fits, shown as solid curves that are compared with experimental data in fig. 4(A).

Fig. 4(B) shows the concentration dependence of specific viscosity, where solid lines are power law fits based on the scaling model in semidilute unentangled (slope of 0.5), semidilute entangled (slope of 1.5) and concentrated regimes (with empirical slope of 2.1). The entanglement concentration  $c_e = 0.053$  M is obtained from the crossover point from semidilute unentangled to entangled, where the concentration exponent triples. These concentration regimes are confirmed by relaxation time as function of concentration. Above ce, the relaxation time becomes independent of concentration as predicted by the scaling theory (eq. 12). In the concentrated regime (c > 0.2 M), the relaxation time has a strong upturn, accompanied by a higher power law exponent in the concentration dependence of specific viscosity. Although the concentrated regime clearly shows a steeper slope than the semidilute entangled regime, higher concentration data would be required to determine a more reliable slope. These phenomena at high solution concentration are observed in other polyelectrolyte solutions and the slope is expected to be 3.75 eventually, as one would expect for entangled neutral polymer solutions. 1, 8, 28 However, there has been limited discussion regarding this strong concentration dependence in concentrated polyelectrolyte solutions and the difference between the semidilute entangled and concentrated regimes, mainly because the oscillatory shear data shown in fig. 4(C) for aqueous solutions do not provide enough information from LVE response; only the terminal regime can be detected from the frequency range applied. There is also an instrument limitation at low frequencies due to the phase angle resolution, as the phase angle is approaching 90° for many aqueous solutions, which restricts us from determining linear viscoelastic relaxation time by extrapolating the G' and G" power laws of  $\omega^2$  and  $\omega^1$ , respectively<sup>23</sup> to where they cross at higher frequency.

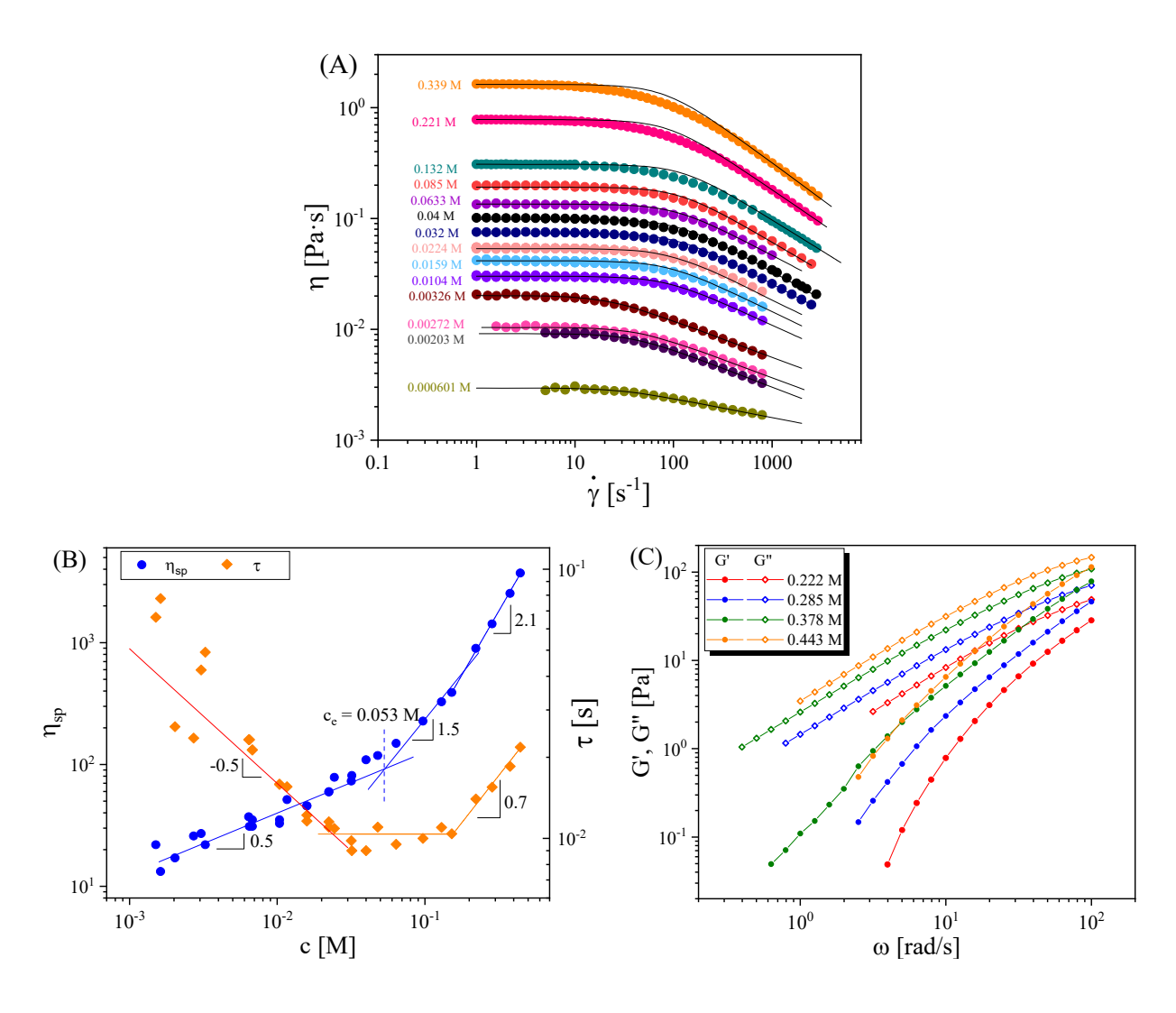


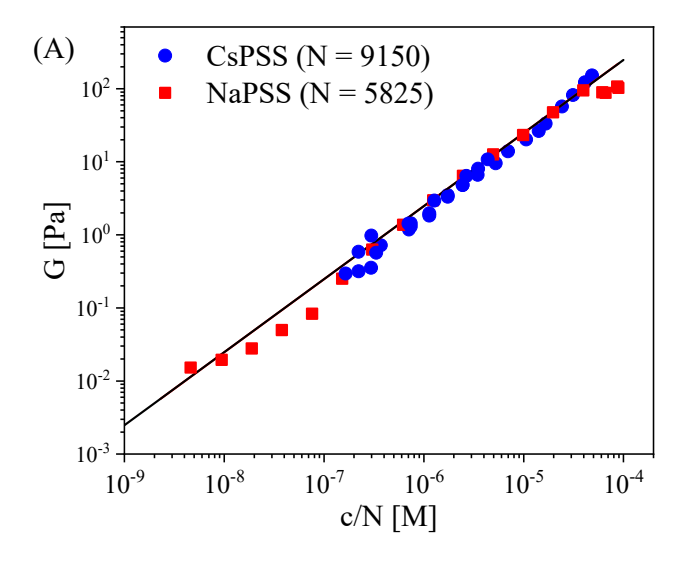
Figure 4. (A)The shear rate dependence of apparent viscosity for CsPSS/water solutions at 25 °C. Each curve is fitted to the Carreau model (solid lines). (B)Concentration dependence of specific viscosity  $\eta_{sp}$  and relaxation time ( $\tau$ ). Solid lines have the slopes predicted by the scaling theory. (C) Oscillatory shear results of high concentration CsPSS/water solutions at 25 °C.

Fig. 5(A) compares the terminal modulus obtained from experiments for NaPSS<sup>1</sup> and the CsPSS aqueous solutions from this study. The line is G = ckT/N, as the Rouse terminal modulus is expected to be kT per chain.<sup>23</sup> Data by Boris and Colby<sup>1</sup> for  $1.2 \times 10^6$  g/mol NaPSS aqueous solutions are also plotted on the same graph to compare with CsPSS.

For the entangled solutions, the tube diameter can be calculated as<sup>23</sup>

$$a = \sqrt{\frac{kT}{G\xi}} \tag{16}$$

where G is the plateau modulus, which is of the order of kT per entanglement strand (eq. 10) and  $\xi$  is the correlation length measured by small angle x-ray scattering. Since plateau modulus cannot be determined from oscillatory shear results in aqueous solutions, terminal modulus is used instead to calculate the tube diameter above  $c_e$ . The tube diameter for both NaPSS and CsPSS has the same concentration dependence as the correlation length, as shown in fig. 5(B).



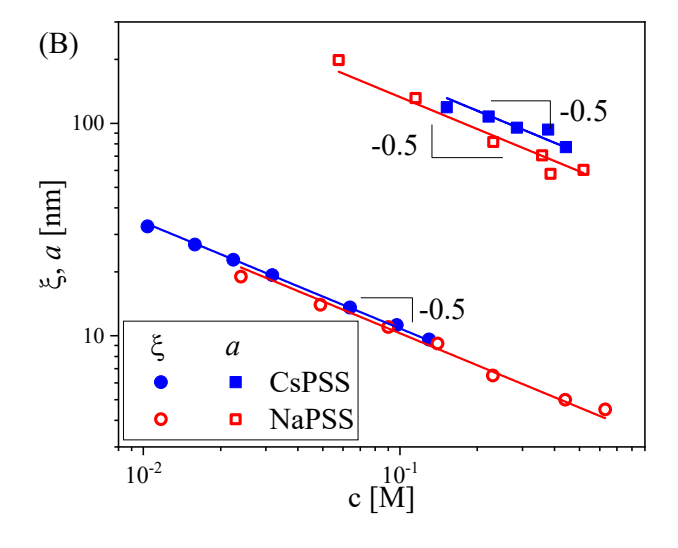


Figure 5. (A) Normalized concentration dependence of terminal moduli at 25 °C for CsPSS/water solutions in this study and NaPSS/water data taken from ref 1. The black solid line is the expectation G = ckT/N. (B) Concentration dependence of correlation length and tube diameter (eq 16) based on terminal modulus for CsPSS/water solutions from this study and NaPSS/water solutions from refs 1 and 39. Both correlation length and tube diameter based on terminal modulus for CsPSS/water solutions exhibit the concentration dependences expected by the scaling model,<sup>3</sup> with  $a \cong 10\xi$ .

CsPSS/EG (anhydrous) solutions. EG has also been used as a solvent for polyelectrolytes. <sup>40</sup> Shear rate dependence of viscosity was used to evaluate  $\eta_{sp}$  and  $\tau$  for partially quaternized poly(2-vinyl pyridine) with chloride counterion in EG and determined that EG is a good solvent for Q-P2VPCI. Ethylene glycol is used in this study because it is 18 times more viscous than water, which slows down the polyelectrolyte solution dynamics. The onset of shear thinning occurs at shear rates between 1 and 10 s<sup>-1</sup> at 25 °C, allowing a good fit of the Carreau model to apparent viscosity data with a wide range of rates for shear thinning as shown in fig. 6(A). The specific viscosity and relaxation time as functions of concentration are plotted in fig. 6(B) and the  $c_e$  is found to be 0.058 M. The terminal modulus, as shown in fig. 6(C), agrees well with the expected values except for the highest concentration, suggesting significant entanglement effects at c = 0.351 M. Using G, the tube diameter is calculated for  $c > c_e$  and fitted to a power law of  $c^{-1/2}$  (fig. 6(D)), as scaling expects  $a \sim \xi$ .

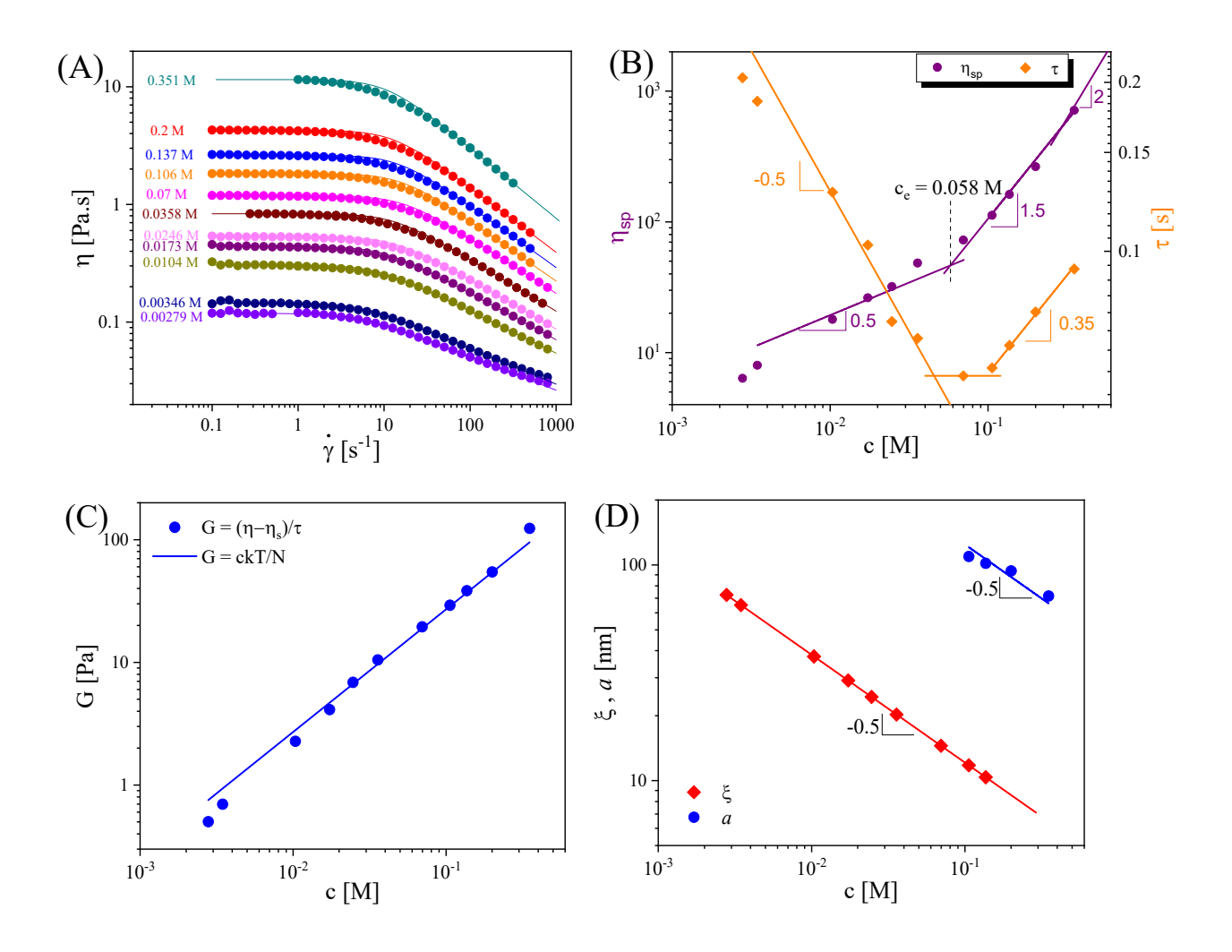


Figure 6. (A) Apparent viscosity as a function of shear rate for CsPSS/anhydrous ethylene glycol solutions at 25 °C are fitted to the Carreau model (eq. 15) as solid curves, where the concentration dependence of specific viscosity( $\eta_{sp}$ ) and relaxation times( $\tau$ ) (shown in B) are obtained. (C) Terminal modulus is calculated for each concentration and compared with the theoretical value of kT per chain, shown as the solid line. (D) The correlation length and tube diameter calculated from terminal modulus (eq. 16) are plotted as functions of concentration, with  $a \cong 10\xi$ .

In principle, oscillatory shear at temperatures above the solution crystallization temperature can be applied to solutions to construct master curves. The melting temperature of EG is -13 °C as reported in Table 1, allowing us to apply the time-temperature superposition (tTS) above -13 °C. However, in order to access the full rubbery plateau shown in fig. 7(A), oscillatory shear experiments need to be performed down to -

25 °C. The addition of polyelectrolyte slows down the crystallization to some extent, but crystallization still slowly occurs on cooling. With crystallization, tTS fails. The van Gurp-Palmen plot (fig. 7(B)) also shows that the tTS fails for CsPSS/EG solutions. Despite the mild failure of tTS, it is clear from fig. 7(A) that only the highest concentration of 0.351 M shows entanglement effects, as the two lower concentrations exhibit no rubbery plateau with G' > G''.

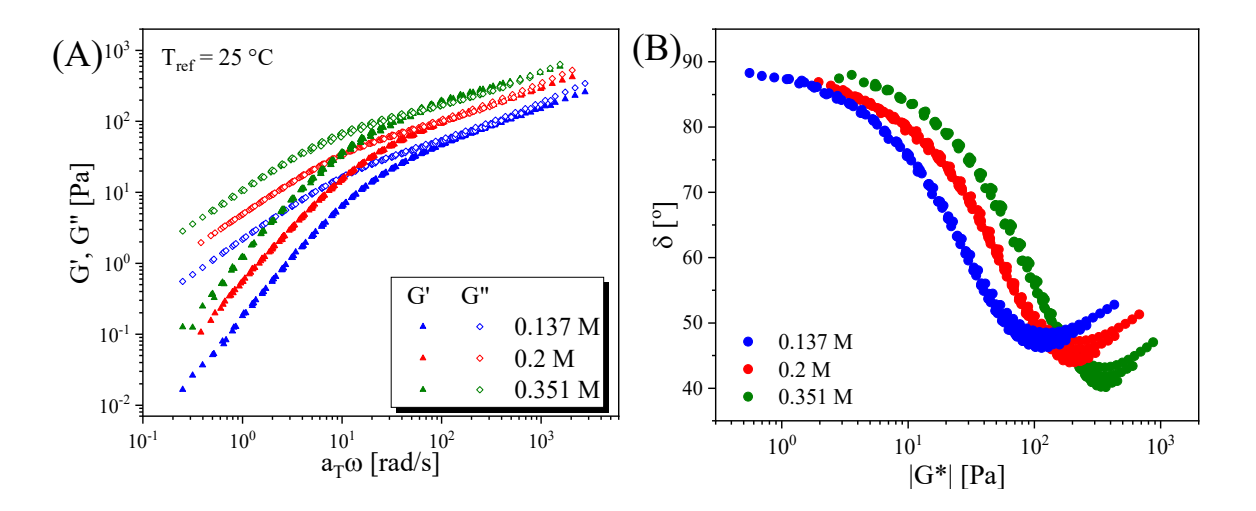


Figure 7. (A)The tTS master curves of CsPSS/anhydrous ethylene glycol solutions are generated from the LVE measurements in the temperature range of 25 °C to -25 °C at reference temperature 25 °C for the highest three concentrations. The highest concentration of 0.351 M is clearly entangled with G' > G" for roughly one decade in frequency. (B) van Gurp-Palmen plot for the same three concentrations of CsPSS/anhydrous EG solutions, showing more clearly the mild failure of tTS.

CsPSS/glycerol (anhydrous) solutions. Due to the constraints on tTS from EG solutions, we use anhydrous glycerol as a solvent because 1) the viscosity of glycerol is >1000 times higher than that of water; 2) glycerol has dielectric constant similar to that of EG and is able to eventually dissolve CsPSS and 3) glycerol can be a supercooled liquid glass-former so that solution crystallization can be effectively avoided.<sup>41</sup>

Glycerol rapidly absorbs substantial amounts of water from the atmosphere. Both viscosity and relaxation time decrease as more water is present in the solution. To avoid the humidity effects on the rheology measurements, solutions are carefully prepared in a glovebox filled with argon gas using anhydrous glycerol. Solutions are loaded quickly onto the measuring geometry and all measurements are under a dry nitrogen blanket. The specific viscosity and relaxation time determined from steady shear experiments, as shown in fig. 8(A), are plotted as functions of concentration and  $c_e$  is determined to be 0.054 M based on the scaling model (fig. 8(B)). In all three solvents, the crossover from  $\eta_{sp} \sim c^{1/2}$  to  $\eta_{sp} \sim c^{3/2}$  yields the same  $c_e$  (0.058 M in fig. 6(B) for ethylene glycol and 0.053 M in fig. 4(B) for water). Thus, according to the scaling theory, concentrations above 0.054 M should all be entangled, which can be tested by their LVE response.

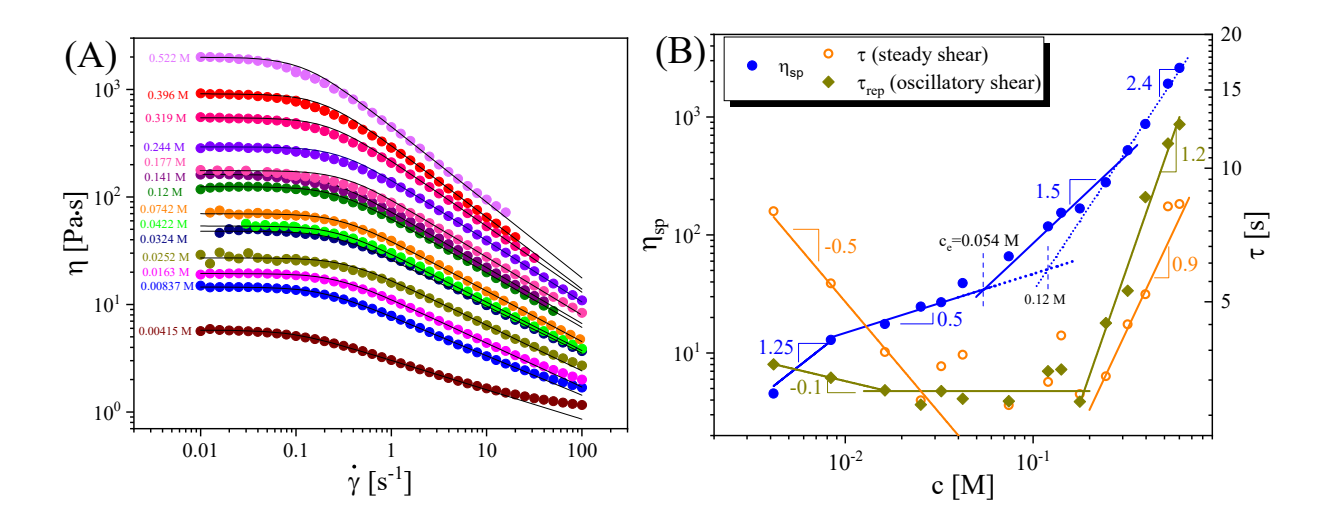


Figure 8. (A) Shear rate dependence of viscosity for CsPSS/anhydrous glycerol at different concentrations at 25 °C. Lines are fits to the Carreau model, eq. 15. (B) Concentration dependences of specific viscosity (blue filled circles) and relaxation time (open orange circles) from the Carreau model fits of part A. Olive diamonds are relaxation times from oscillatory shear at 25 °C as  $\tau_{rep}$ , the reciprocal of the frequency where G' = G'' at the low frequency end of the rubbery plateau.

**Linear viscoelastic response.** To understand the entanglement of polyelectrolyte solutions, master curves are generated from the oscillatory shear experiments from 25 °C to -5 °C and presented in fig. 9(A). tTS is found to work nicely for CsPSS/glycerol solutions based on the van Gurp-Palmen plots shown in fig. 9(B).

Utilizing the master curves provides a great way of verifying the true  $c_e$  as the emergence of a rubbery plateau where G' and G" cross each other twice. For example, the 0.12 M solution shows entangled LVE response although the rubbery plateau is very narrow. From these master curves, one can clearly tell that the 0.0742 M solution is not entangled, as G" is always greater than G'. The frequency where G' = G'' at the low frequency end of the rubbery plateau is taken to be the inverse of the reptation time  $(1/\tau_{rep})$  and that at high frequency is the inverse of the Rouse time of an entanglement strand  $(1/\tau_e)$ . The plateau width can then be calculated as  $\tau_{rep}/\tau_e$ , where the  $c_e$  of 0.106 M is determined by extrapolating the power law concentration dependence of  $\tau_{rep}/\tau_e$  to unity in fig. 10(A), and this  $c_e$  is a factor of 2 higher than that obtained from the scaling model. The fact that the scaling model underestimates  $c_e$  is tested by oscillatory shear experiments. Based on the scaling model prediction of  $c_e = 0.054$  M in fig. 8(B), the higher concentration of 0.0742 M solution should be well entangled ( $c/c_e = 1.4$ ), but its master curve clearly shows an unentangled LVE response, shown as the lowest (orange) data set in fig. 9(A).

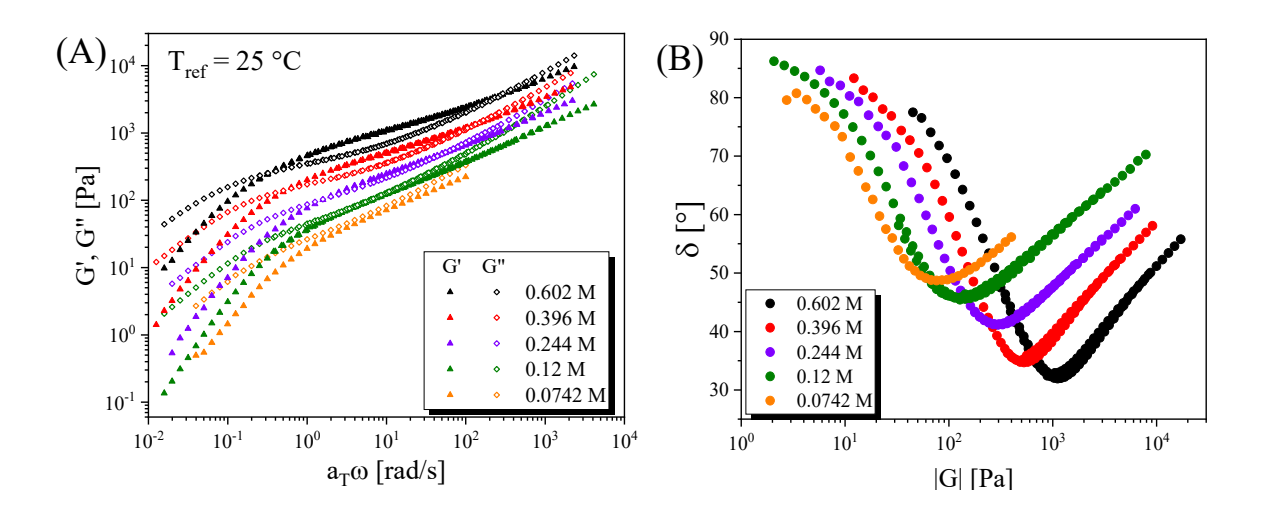


Figure 9. (A) Master curves of CsPSS/glycerol with reference temperature at 25 °C with oscillatory shear experiments performed between 25 °C and -5 °C. (B) van Gurp-Palmen plot of CsPSS/glycerol solutions at various concentrations, showing that tTS works better for the glycerol solutions than for the EG solutions in fig. 7B.

Additionally, the concentration dependence of  $\eta_{sp}$  varies as  $c^{2.4}$  at concentrations above 0.28 M, which is a common feature for most polyelectrolyte solutions in the well entangled regime.<sup>1, 9, 28</sup> Interestingly, the crossover between  $\eta_{sp} \sim c^{2.4}$  and the semidilute unentangled regime gives an estimate of  $c_e = 0.12$  M which is much closer to the real  $c_e = 0.106$  M.

Figure 10(A) compares the plateau width of CsPSS/glycerol with some neutral polymer solutions from the literature, where concentrations are normalized by  $c_e$  of each system so that all datasets are reduced to a universal power law with an exponent of 4, which is not consistent with the exponent 3/2 expected for entangled polyelectrolyte solutions with no salt. As presented in eq. 5, the plateau width  $\tau_{rep}/\tau_e$  shows the concentration dependence of  $c^4$  expected for flexible neutral polymer solutions regardless of solvent quality (eq. 5).<sup>26</sup> We find that the plateau width of CsPSS/glycerol also falls on the same power law as all the neutral polymer solutions, which reveals that entangled polyelectrolyte solutions are similar to neutral polymer solutions. The shape of the master curve of 247 kg/mol polystyrene/ethylbenzene solution at 5.58 M is compared with that of 0.522 M CsPSS/glycerol in fig. 10(B). The two concentrations are chosen to be  $5c_e$  as indicated by the black circle in fig. 10(A). By reducing the modulus scale and frequency scale by  $G_e$  and  $\tau_e$ , the two master curves (both at reference temperature 25 °C) adopt identical shapes as they are nearly perfectly overlapping each other.

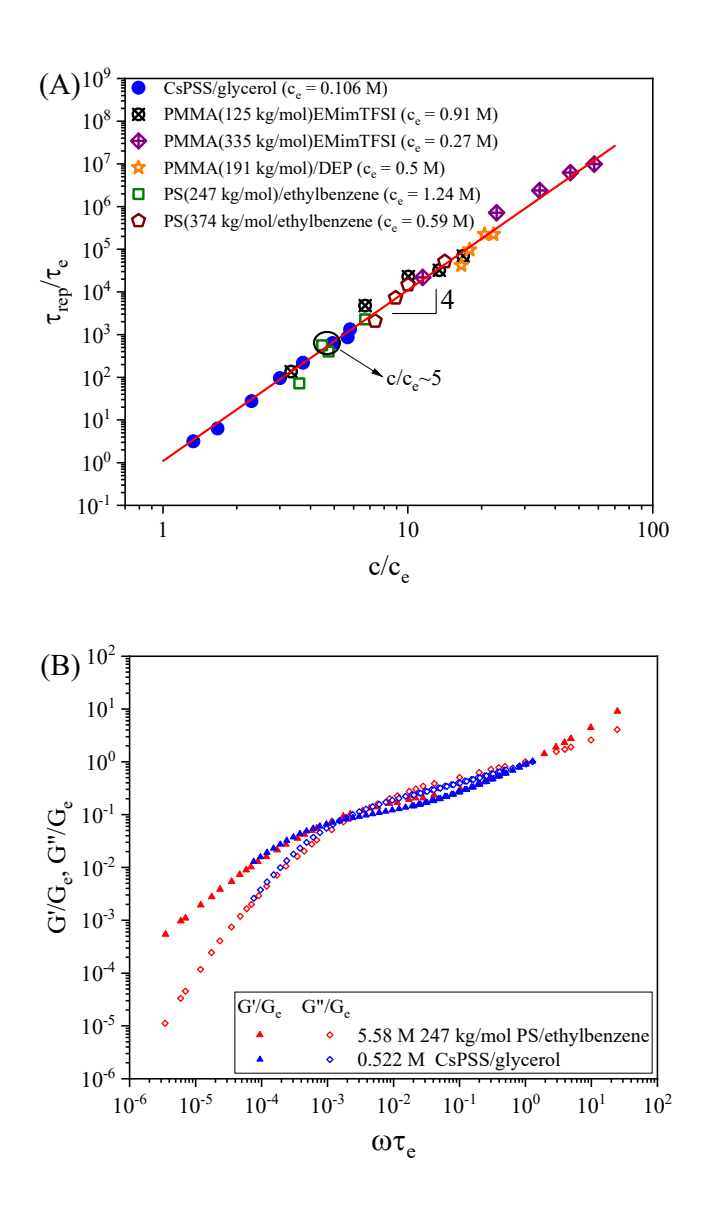


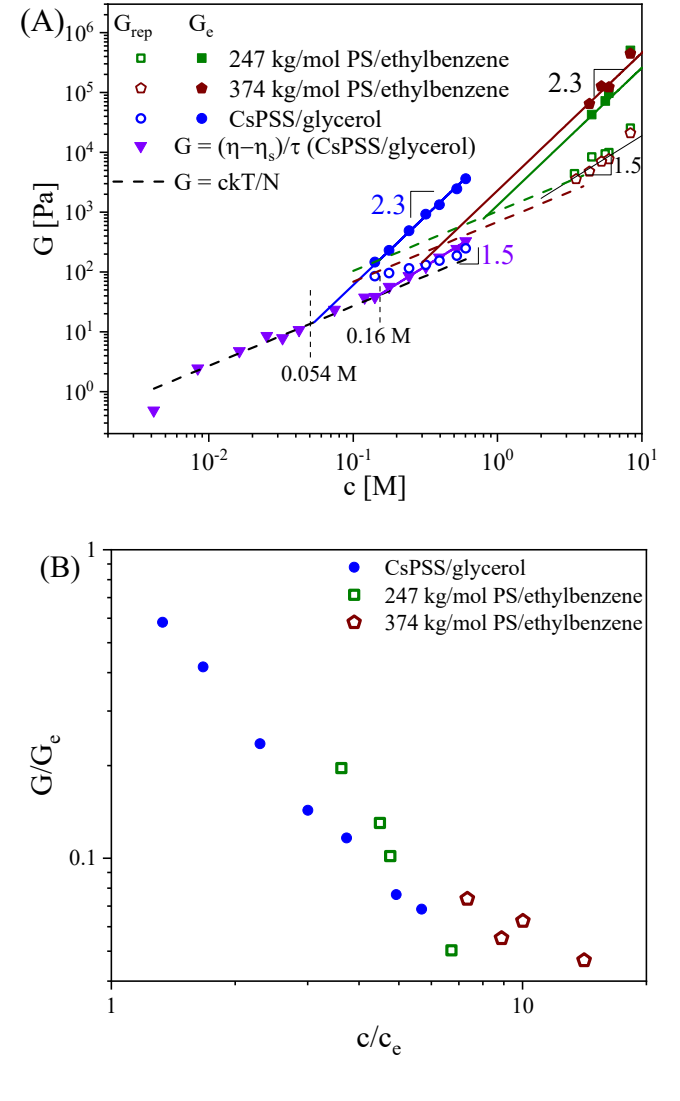
Figure 10. (A) Plateau width  $\tau_{rep}/\tau_e$  as a function of concentration normalized by entanglement concentration  $c_e$  of each polymer solution (listed in the Legend), including CsPSS/glycerol from this study and literature data taken from refs 26, 42 and 43 for neutral polymer solutions. The solid line is a power law fit with the exponent of 4, expected for neutral polymer solutions (eq. 5). (B) Comparison of master curves of 5.58 M 247 kg/mol polystyrene/ethylbenzene and 0.522 M CsPSS/glycerol. The two concentrations are chosen at  $c \approx 5c_e$  (black circle in panel A). Modulus and frequency are reduced by  $G_e$  and  $\tau_e$ , respectively. The conclusion is that entangled CsPSS/glycerol solutions exhibit nearly identical LVE as entangled solutions of neutral polymers.

Moreover, we assessed the tube diameter by taking the plateau modulus  $G_e$  from each master curve as the modulus value at the high frequency crossing of G' and G''. The concentration dependence of  $G_e$  is quite different from that of terminal modulus as shown in fig. 11(A) for both entangled polyelectrolyte solutions and neutral polymer solutions. The power law fit of  $G_e$  agrees with neutral polymer solutions in both  $\theta$  and good solvents as  $G_e \sim e^{2.3}$  (eq. 2) as shown in fig. 11(A).<sup>6,23</sup> Extrapolating  $G_e \sim e^{2.3}$  back to the black dashed line (G = ckT/N) gives  $c_e = 0.054$  M which is the same as the  $c_e$  from the concentration dependence of  $\eta_{sp}$  changing from  $e^{1/2}$  to  $e^{3/2}$ . The crossover point is roughly half of the  $e_e$  from extrapolating  $\tau_{rep}/\tau_e$  to unity (0.106 M). Different  $e_e$  values from the two extrapolations are also observed for entangled neutral polymer solutions. Fig. 11(A) shows  $e_e$  of PS/ethylbenzene solutions determined by extrapolating  $e_e \sim e^{2.3}$  to  $e_e \sim c^{2.3}$  for PS/ethylbenzene. Such a difference is hardly surprising, since neither  $e_e \sim c^{2.3}$  are precisely where  $e_e \sim c^{2.3}$  for PS/ethylbenzene.

The different concentration dependences of G and  $G_e$  are observed for both CsPSS/glycerol and PS/ethylbenzene. The ratio  $G/G_e$  as a function of  $c/c_e$  for CsPSS/glycerol is comparable with that of PS/ethylbenzene solutions shown in fig. 11(B).  $G/G_e$  gradually decreases with increasing concentration as more relaxation modes are present in the widening rubbery plateau. The scaling model for neutral polymer solutions works nicely for describing the concentration dependence of plateau modulus  $G_e$  (eq. 2). However, fig. 11(B) shows that the terminal modulus G needs to have weaker concentration dependence, curiously more like the  $G \sim c^{3/2}$  expected for the plateau modulus  $G_e$  (not the terminal modulus G) of entangled polyelectrolyte solutions. LVE of narrow molecular weight distribution linear polymers have their low frequency crossing of G' and G" coincide with the local maximum in the loss moduls  $G''_{max}$ , so that terminal modulus  $G = G''_{max}$ . In the literature, this terminal modulus is recognized to be smaller than the plateau modulus, but the two are often assumed to be proportional ( $G_e = \alpha G$ ) with  $\alpha = 4.83$  proposed by Oser and

Marvin<sup>44</sup> and  $\alpha = 3.56$  proposed by Raju, et al.<sup>45</sup> Fig. 11(B) shows clearly that G/G<sub>e</sub> is not at all constant for concentrations less than  $10c_e$ .

Fig. 11(A) shows that the terminal modulus G initially agrees with kT per chain in the unentangled regime and starts to have a stronger concentration dependence above  $c_e$  which is the power law of  $c^{3/2}$  expected by the scaling theory.<sup>3</sup> As shown in fig. 11(C), if terminal modulus is used to calculate the tube diameter, the concentration dependence of tube diameter scales as  $c^{-1/2}$  which is also observed in water and EG solutions, whereas a smaller  $a \sim c^{-0.92}$  is obtained if the larger  $G_e$  is used (blue data in fig. 11(C)). If using G instead to calculate a, the concentration dependence of a for CsPSS/glycerol is the same as that for CsPSS/water in fig. 5(B) and CsPSS/EG in fig. 6(D), with  $a \sim \xi \sim c^{-0.5}$ .



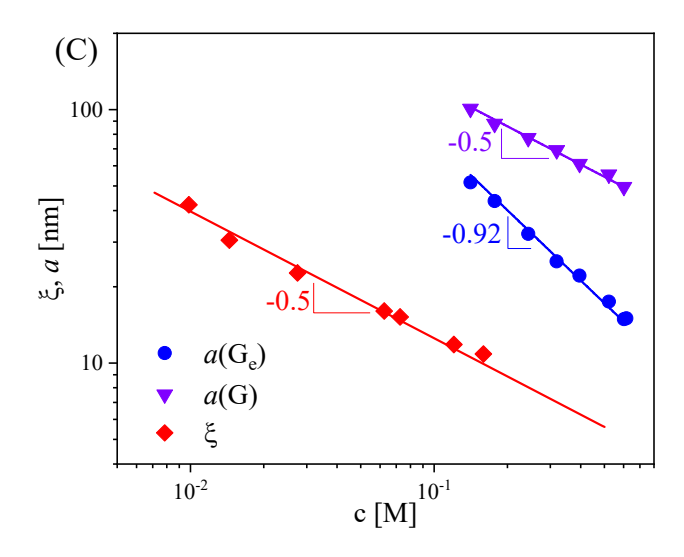


Figure 11. (A). Comparing  $G = (\eta - \eta_s)/\tau$  from Carreau model fits to shear thinning viscosity data,  $G_{rep}$  (the low frequency crossing of G' and G'') and  $G_e$  (the high frequency crossing of G' and G'') of CsPSS/glycerol with polystyrene/ethylbenzene solutions.  $G_{rep}$  is measured as the low frequency crossing of G' and G''. The dashed lines represent the theoretical moduli calculated as G = ckT/N for unentangled concentrations, where degree of polymerization N = 2375 for 247 kg/mol PS and N = 3596 for 374 kg/mol PS. The crossover from G = ckT/N to  $G_e \sim c^{2.3}$  is 0.85 M for 247 kg/mol PS/ethylbenzene (red pentagons), and 0.39 M for 374 kg/mol PS/ethylbenzene (green squares). (B) Ratio of terminal modulus and plateau modulus  $G/G_e$  as a function of  $c/c_e$ . (C) Tube diameter of CsPSS/glycerol solutions determined by eq. 16 using  $G_e$  (blue circles) and by eq. 16 using  $G_e$  (violet triangles) and correlation length (red diamonds) as functions of concentration. Solid lines are power law fits. Again with  $a \cong 10\xi$  for the tube diameter calculated from terminal modulus.

Figure 12 plots  $kT/G\xi^3$  as a function of concentration in all three solvents, which shows two regimes. In the unentangled regime,  $kT/G\xi^3 \sim c^{1/2}$  since  $G \sim c$  and  $\xi \sim c^{-1/2}$ . In the entangled regime,  $kT/G\xi^3 = P_e^2$  (the square of the entanglement overlap parameter, eq. 9) and becomes independent of concentration as it should, since the concentration dependence of terminal modulus changes to  $G \sim c^{3/2}$ , and  $P_e$  values for different systems are obtained from this regime. The crossover from  $P_e^2 \sim c^{1/2}$  to  $e^0$  gives  $e^0 = 0.16$  M for CsPSS/glycerol, which is the same as the crossover from  $e^0 \sim c^{1/2}$  to  $e^0$  gives  $e^0 = 0.16$  M. This gives a

closer approximation of  $c_e$  to our estimate of  $c_e$  from extrapolating  $\tau_{rep}/\tau_e$  to unity (0.106 M) than the crossover concentration where the specific viscosity exponent triples (0.054 M).

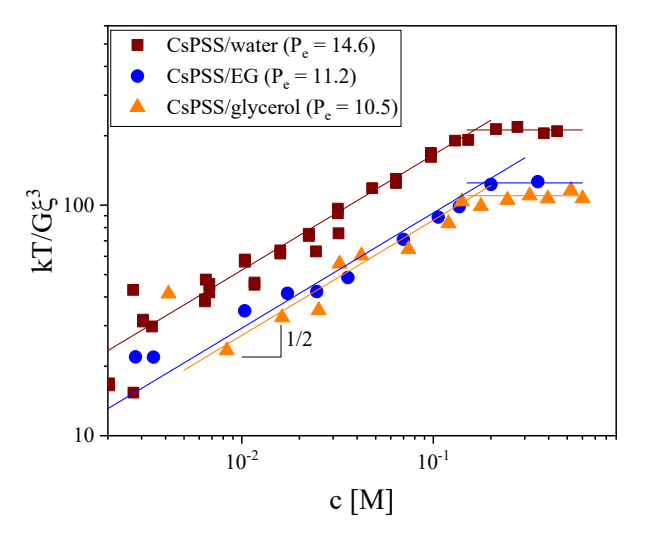


Figure 12. The square of entanglement overlap parameter  $P_e^2 = kT/G\xi^3$  of CsPSS in three different solvents as a function of concentration. For entangled solutions with  $c > c_e$ ,  $P_e$  is expected to be constant (with values listed in the Legend) while for unentangled solutions with  $c < c_e$ ,  $kT/G\xi^3 \approx N/g$ , the number of correlation blobs per chain.

Table 2. Entanglement concentrations determined using four different methods

	c <sub>e</sub> [M] from						
	$\eta_{ ext{sp}}$	Pe	$ au_{rep}/ au_{e}$	Ge			
CsPSS/water	0.053	0.17					
CsPSS/EG	0.058	0.18					
CsPSS/glycerol	0.054	0.16	0.106	0.054			
247 kg/mol PS/ethylbenezene			1.24	0.85			
374 kg/mol PS/ethylbenzene			0.59	0.39			

A great question that we currently cannot answer is: Above what concentration ( $c_D$ ) should polyelectrolytes lose their charge effects? This crossover concentration should be where the correlation length reaches the electrostatic blob size. Since the latter is expected to be of order 1 nm for strongly charged polyelectrolytes with condensed counterions,  $^4$   $c_D$  should be considerably larger than any concentration studied herein. Our scattering data still show a polyelectrolyte correlation peak at 0.16 M (fig. 2) placing a lower bound on  $c_D$ . Entanglement effects in polyelectrolyte solutions seem to be seen in different measured properties at different apparent  $c_e$  that are summarized in Table 2. The lowest  $c_e$  is from the power law concentration dependence of specific viscosity changing from unentangled  $\eta_{sp} \sim c^{1/2}$  to  $\eta_{sp} \sim c^{3/2}$ . That is roughly a factor of 2 smaller than the estimate of  $c_e$  from extrapolating  $\tau_{rep}/\tau_e$  to unity. So perhaps the apparent scaling of  $\eta_{sp} \sim c^{3/2}$  is actually a broader-than-expected crossover to the truly entangled solution with  $\eta_{sp} \sim c^{2.4}$ .

Universal concentration dependence of power law index. Jouenne and Levache<sup>46</sup> found that the power law indices have a universal concentration dependence after normalizing with the overlap concentration c\* for various neutral polymer solutions. For polyelectrolyte solutions, the overlap concentration c\* is defined in eq. 7 and using eq. 14, the normalized concentration can be expressed as  $\frac{c}{c^*} = \frac{N^2}{c^2 \xi^6}$ . Note that this form does not care about the choice of "monomer", since c/N is the number density of chains. By plotting the power law index n as a function of normalized concentration in fig. 13, all n values of different solvents nicely follow a universal decrease as concentration is raised, with no change in the trend noted at c<sub>e</sub>.

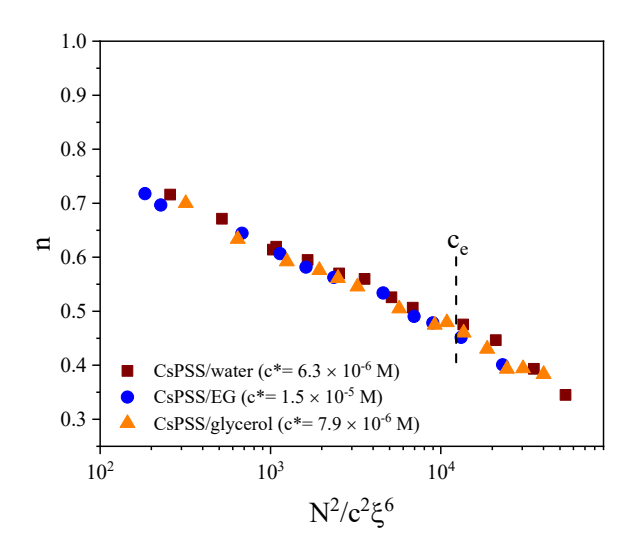


Figure 13. Power law index from the Carreau model fits (defined in eq. 10, which at high shear rates has  $\eta \sim \dot{\gamma}^{n-1}$ ) as a function of concentration reduced by the overlap concentration (c\*) since  $\frac{c}{c^*} = \frac{N^2}{c^2 \xi^6}$  for CsPSS in three solvents.

#### 4. Conclusions

We have studied the rheology of salt-free CsPSS/glycerol solutions and examined the dynamic properties of polyelectrolyte solutions from their LVE response that cannot be observed in aqueous solutions with our rheometers. By extrapolating the rubbery plateau width to unity, a more accurate entanglement concentration  $c_e$  is obtained, which is greater than the  $c_e$  determined from the scaling theory, suggesting that the use of the scaling theory where  $\eta_{sp} \sim c^{1/2}$  crosses to  $\eta_{sp} \sim c^{3/2}$  underestimates the true entanglement concentration. This observation suggests that the well-recognized semidilute entangled concentration regime where  $\eta_{sp} \sim c^{3/2}$  might be a broad crossover between unentangled dynamics described by the Rouse model with  $\eta_{sp} \sim c^{1/2}$  and entangled dynamics described by the reptation model.

The semidilute unentangled regime covers many decades in concentration for polyelectrolytes with no salt, since the coil size shrinks faster as concentration is increased ( $R \sim c^{-1/4}$ ) compared with neutral polymers in good solvent ( $R \sim c^{-1/8}$ ). That effectively pushes the entanglement concentration higher and for CsPSS in

glycerol, ethylene glycol and water, makes the crossover to neutral polymer scaling apparently occur

slightly below the true entanglement concentration. Hence entangled solutions of CsPSS behave as neutral

polymer solutions.

We also found that the entanglement overlap parameter  $P_e = 10.5$  for entangled CsPSS/glycerol, which is

comparable with entanglement overlap parameters of neutral polymer solutions. The scaling theory

(predicting  $\eta_{sp} \sim c^{3/2}$  in eq. 11 and  $\tau \sim c^0$  in eq. 12) still works for polyelectrolyte solutions near entanglement

in a very narrow concentration range. However, once the concentration is above the real ce, the solutions

behave as entangled neutral polymer solutions. For future studies, salt-free solutions of polyelectrolytes

with different molecular weights need to be systematically examined to provide insights regarding the chain

length dependence of entanglement concentration c<sub>e</sub> and to prove that G<sub>e</sub> does not depend on chain length.

Also very useful would be study of a high molecular weight polyelectrolyte in a solvent for which the

neutral form of that polymer is also soluble, as then the electrostatic blob should be larger (and c<sub>D</sub> smaller).

**Author Information** 

**Corresponding Author** 

\*Ralph H. Colby

Department of Materials Science and Engineering, Pennsylvania State University, University Park,

Pennsylvania 16802, United States;

Email rhc@plmsc.psu.edu

Tel +1-814-863-3457

**ORCID** 

32

Aijie Han <a href="https://orcid.org/0000-0002-9309-5912">https://orcid.org/0000-0002-9309-5912</a>

Ralph H. Colby <a href="https://orcid.org/0000-0002-5492-6189">https://orcid.org/0000-0002-5492-6189</a>

Acknowledgments

This research is funded by the National Science Foundation Chemistry-1904852. We thank Sintu Rongpipi for making the synchrotron SAXS measurements in glycerol. We also thank Prof. Andrey Dobrynin for helpful discussions.

**Supporting Information** 

Terminal modulus and tube diameter of CsPSS in three solvents compared with plateau modulus in glycerol; Cox-Merz relationship of three entangled and two unentangled CsPSS/glycerol solutions.

#### References

- 1. Boris, D. C.; Colby, R. H. Rheology of Sulfonated Polystyrene Solutions. *Macromolecules* **1998**, 31 (17), 5746-5755.
- 2. De Gennes, P. G. Dynamics of Entangled Polymer Solutions. I. The Rouse Model. *Macromolecules* **1976**, 9 (4), 587-593.
- 3. Dobrynin, A. V.; Colby, R. H.; Rubinstein, M. Scaling Theory of Polyelectrolyte Solutions. *Macromolecules* **1995**, 28 (6), 1859-1871.
- 4. Dobrynin, A. V.; Rubinstein, M. Theory of polyelectrolytes in solutions and at surfaces. *Progress in Polymer Science* **2005**, 30 (11), 1049-1118.
- 5. Krause, W. E.; Tan, J. S.; Colby, R. H. Semidilute solution rheology of polyelectrolytes with no added salt. *Journal of Polymer Science Part B: Polymer Physics* **1999**, 37 (24), 3429-3437.
- 6. Colby, R. H. Structure and linear viscoelasticity of flexible polymer solutions: comparison of polyelectrolyte and neutral polymer solutions. *Rheologica Acta* **2010**, 49 (5), 425-442.
- 7. Kaji, K.; Urakawa, H.; Kanaya, T.; Kitamaru, R. Phase diagram of polyelectrolyte solutions. *J Phys-Paris* **1988**, 49.
- 8. Dou, S.; Colby, R. H. Charge density effects in salt-free polyelectrolyte solution rheology. *Journal of Polymer Science Part B: Polymer Physics* **2006**, 44 (14), 2001-2013.
- 9. Dou, S.; Colby, R. H. Solution Rheology of a Strongly Charged Polyelectrolyte in Good Solvent. *Macromolecules* **2008**, 41 (17), 6505-6510.
- 10. Fuoss, R. M. Viscosity function for polyelectrolytes. *Journal of Polymer Science* **1948,** 3 (4), 603-604.
- 11. Fuoss, R. M.; Strauss, U. P. Polyelectrolytes. II. Poly-4-vinylpyridonium chloride and poly-4-vinyl-N-n-butylpyridonium bromide. *Journal of Polymer Science* **1948**, 3 (2), 246-263.
- 12. Fuoss, R. M. Polyelectrolytes. *Discussions of the Faraday Society* **1951**, 11 (0), 125-134.
- 13. Dobrynin, A. Theory and simulations of charged polymers: From solution properties to polymeric nanomaterials. *Current Opinion in Colloid & Interface Science* **2008**, 13, 376-388.
- 14. Lopez, C. G. Entanglement of semiflexible polyelectrolytes: Crossover concentrations and entanglement density of sodium carboxymethyl cellulose. *Journal of Rheology* **2020**, 64 (1), 191-204.
- 15. Lopez, C. G.; Colby, R. H.; Cabral, J. T. Electrostatic and Hydrophobic Interactions in NaCMC Aqueous Solutions: Effect of Degree of Substitution. *Macromolecules* **2018**, 51 (8), 3165-3175.
- 16. Dukhin, A. S.; Goetz, P. J. Bulk viscosity and compressibility measurement using acoustic spectroscopy. *The Journal of Chemical Physics* **2009**, 130 (12), 124519.
- 17. Schroyen, B.; Vlassopoulos, D.; Van Puyvelde, P.; Vermant, J. Bulk rheometry at high frequencies: a review of experimental approaches. *Rheologica Acta* **2020**, 59 (1), 1-22.
- 18. Doi, M.; Edwards, S. F. Dynamics of concentrated polymer systems. Part 1.—Brownian motion in the equilibrium state. *Journal of the Chemical Society, Faraday Transactions 2: Molecular and Chemical Physics* **1978**, 74 (0), 1789-1801.
- 19. Doi, M.; Edwards, S. F. Dynamics of concentrated polymer systems. Part 2.—Molecular motion under flow. *Journal of the Chemical Society, Faraday Transactions 2: Molecular and Chemical Physics* **1978,** 74 (0), 1802-1817.
- 20. Doi, M.; Edwards, S. F. Dynamics of concentrated polymer systems. Part 3.—The constitutive equation. *Journal of the Chemical Society, Faraday Transactions 2: Molecular and Chemical Physics* **1978**, 74 (0), 1818-1832.
- 21. Heo, Y.; Larson, R. G. Universal Scaling of Linear and Nonlinear Rheological Properties of Semidilute and Concentrated Polymer Solutions. *Macromolecules* **2008**, 41 (22), 8903-8915.
- 22. Heo, Y.; Larson, R. G. The scaling of zero-shear viscosities of semidilute polymer solutions with concentration. *Journal of Rheology* **2005**, 49 (5), 1117-1128.
- 23. Rubinstein, M.; Colby, R. H., *Polymer Physics*. Oxford University Press: 2003.

- 24. Fetters, L. J.; Lohse, D. J.; Colby, R. H. Chain Dimensions and Entanglement Spacings: Datasheet from · Volume : "Physical Properties of Polymers Handbook" in SpringerMaterials, Springer Science+Business Media, LLC.
- 25. Graessley, W. W.; Edwards, S. F. Entanglement interactions in polymers and the chain contour concentration. *Polymer* **1981**, 22 (10), 1329-1334.
- 26. Baumgärtel, M.; Willenbacher, N. The relaxation of concentrated polymer solutions. *Rheologica Acta* **1996**, 35 (2), 168-185.
- 27. Manning, G. S. Counterion binding in polyelectrolyte theory. *Accounts of Chemical Research* **1979**, 12 (12), 443-449.
- 28. Lopez, C. G.; Rogers, S. E.; Colby, R. H.; Graham, P.; Cabral, J. T. Structure of sodium carboxymethyl cellulose aqueous solutions: A SANS and rheology study. *Journal of Polymer Science Part B: Polymer Physics* **2015**, 53 (7), 492-501.
- 29. Edwards, S. F. The theory of polymer solutions at intermediate concentration. *Proceedings of the Physical Society* **1966**, 88 (2), 265-280.
- 30. Fetters, L. J.; Lohse, D. J.; Colby, R. H., Chain Dimensions and Entanglement Spacings. In *Physical Properties of Polymers Handbook*, Mark, J. E., Ed. Springer New York: New York, NY, 2007; pp 447-454.
- 31. Prini, R. F.; Lagos, A. E. Tracer diffusion, electrical conductivity, and viscosity of aqueous solutions of polystyrenesulfonates. *Journal of Polymer Science Part A: General Papers* **1964,** 2 (6), 2917-2928.
- 32. Oostwal, M. G.; Blees, M. H.; De Bleijser, J.; Leyte, J. C. Chain self-diffusion in aqueous salt-free solutions of sodium poly(styrenesulfonate). *Macromolecules* **1993**, 26 (26), 7300-7308.
- 33. Barba, C.; Montané, D.; Farriol, X.; Desbrières, J.; Rinaudo, M. Synthesis and characterization of carboxymethylcelluloses from non-wood pulps II. Rheological behavior of CMC in aqueous solution. *Cellulose* **2002**, 9 (3-4), 327-335.
- 34. Lopez, C. G.; Colby, R. H.; Graham, P.; Cabral, J. T. Viscosity and Scaling of Semiflexible Polyelectrolyte NaCMC in Aqueous Salt Solutions. *Macromolecules* **2017**, 50 (1), 332-338.
- 35. Daubert, T. E., Physical and thermodynamic properties of pure chemicals : data compilation. Danner, R. P., Ed.
- 36. Lide, D. R., CRC handbook of thermophysical and thermochemical data. Kehiaian, H. V., Ed.
- 37. Herbst, C. A.; Cook, R. L. High-pressure viscosity of glycerol measured by centrifugal-force viscometry. *Nature* **1993**, 361 (6412), 518-520.
- 38. De Gennes, P. G.; Pincus, P.; Velasco, R. M.; Brochard, F. Remarks on Polyelectrolyte Conformation. *J Phys-Paris* **1976**, 37 (12), 1461-1473.
- 39. Nierlich, M.; Williams, C. E.; Boue, F.; Cotton, J. P.; Daoud, M.; Farnoux, B.; Jannink, G.; Picot, C.; Moan, M.; Wolff, C.; Rinaudo, M.; Gennes, P. G. D. Small-Angle Neutron-Scattering by Semi-Dilute Solutions of Polyelectrolyte. *J Phys-Paris* **1979**, 40 (7), 701-704.
- 40. Ermi, B. D.; Amis, E. J. Influence of Backbone Solvation on Small Angle Neutron Scattering from Polyelectrolyte Solutions. *Macromolecules* **1997**, 30 (22), 6937-6942.
- 41. Schröter, K.; Donth, E. Viscosity and shear response at the dynamic glass transition of glycerol. *The Journal of Chemical Physics* **2000**, 113 (20), 9101-9108.
- 42. Mok, M. M.; Liu, X.; Bai, Z.; Lei, Y.; Lodge, T. P. Effect of Concentration on the Glass Transition and Viscoelastic Properties of Poly(methyl methacrylate)/Ionic Liquid Solutions. *Macromolecules* **2011**, 44 (4), 1016-1025.
- 43. Masuda, T.; Toda, N.; Aoto, Y.; Onogi, S. Viscoelastic Properties of Concentrated Solutions of Poly(methyl methacrylate) in Diethyl Phthalate. *Polymer Journal* **1972**, 3 (3), 315-321.
- 44. Oser, H.; Marvin, R.S. Effect of molecular weight on viscoelastic properties of polymers as predicted by a molecular theory. *Journal of Research of the National Bureau of Standards* **1963**, 67B (2), 87-90.

- 45. Raju, V. R.; Menezes, E. V.; Marin, G.; Graessley, W. W.; Fetters, L. J. Concentration and molecular weight dependence of viscoelastic properties in linear and star polymers. *Macromolecules* **1981**, 14 (6), 1668-1676.
- 46. Jouenne, S.; Levache, B. Universal viscosifying behavior of acrylamide-based polymers used in enhanced oil recovery. *Journal of Rheology* **2020**, 64 (5), 1295-1313.

# **Supporting Information**

# **Rheology of Entangled Polyelectrolyte Solutions**

Aijie Han and Ralph H. Colby\*

Materials Science and Engineering and Materials Research Institute,

Pennsylvania State University, University Park, PA 16802

Comparisons of CsPSS in three different solvents. The solvent effects mainly change the correlation length due to different dielectric constants. The terminal modulus (G) as shown in Fig. S1 is identical for different solvents for unentangled solutions, as G is always kT per chain (the line is ckT/N). The tube diameter of entangled solutions extracted from G changes with solvents because it is related to the correlation length (Eq. 16 in the paper) which depends on the dielectric constant of solvents. The concentration dependence of tube diameter is  $e^{-0.5}$  (Fig. S2) if the terminal modulus is used to calculate e0 using Eq. (16) because e0 constant of solvents in the entangled regime.

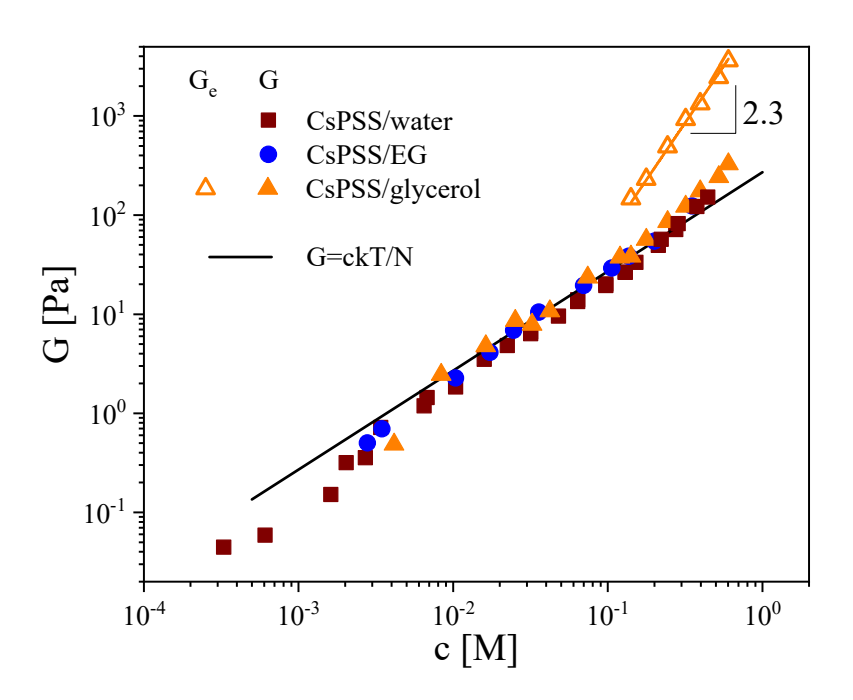
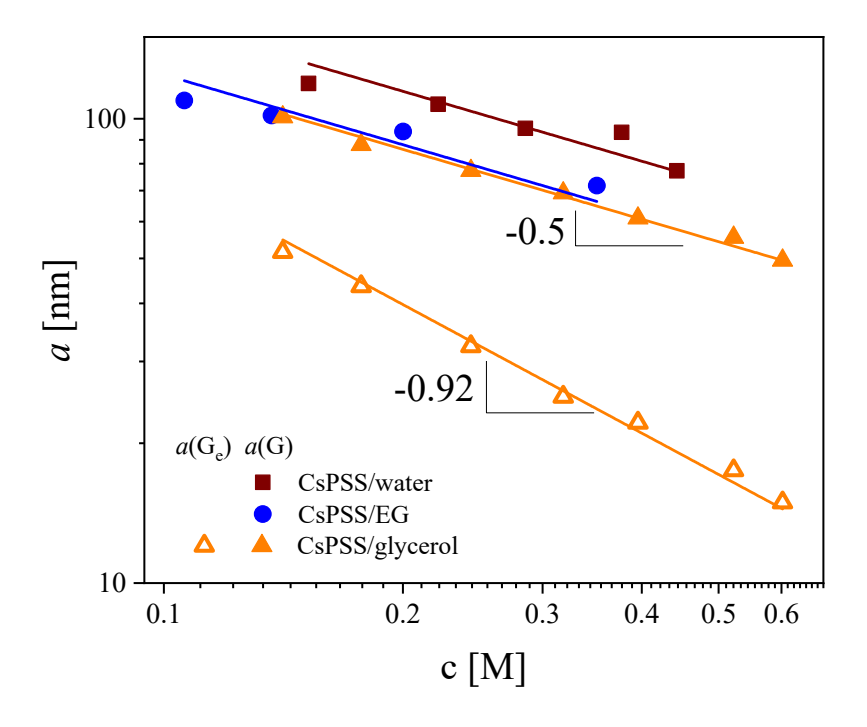


Figure S1. Comparison of terminal modulus G at 25 °C for CsPSS ( $M_n = 2.83 \times 10^6$  g/mol) in three solvents (filled symbols) and the high frequency plateau modulus  $G_e$  in glycerol (open symbols).

<sup>\*</sup>corresponding author rhc@plmsc.psu.edu



**Figure S2.** Comparison of tube diameter estimated from plateau moduli  $(a(G_e) = (kT/G_e\xi)^{1/2}$ , open symbols) in glycerol and terminal moduli  $(a(G) = (kT/G\xi)^{1/2}$ , filled symbols) at 25 °C of CsPSS (M<sub>n</sub> =  $2.83 \times 10^6$  g/mol) in three solvents.

The tube diameter estimated from terminal modulus G is larger than but proportional to the correlation length  $(a \sim \xi \sim c^{-1/2})$  for polyelectrolyte solutions without salt. The tube diameter estimated from the larger plateau modulus  $G_e$  is larger than the correlation length and smaller than the tube diameter estimated from terminal modulus G, with a stronger concentration dependence since  $G_e \sim c^{2.3}$ .

Cox-Merz comparison for CsPSS/glycerol solutions. The empirical Cox-Merz rule expects the steady shear viscosity at any shear rate  $\dot{\gamma}$  to be identical to the magnitude of the complex viscosity at an angular frequency  $\omega = \dot{\gamma}$ . This rule is tested for five CsPSS/glycerol solutions in Fig. S3, where only the three highest concentrations are entangled solutions. The Cox-Merz rule is found to work reasonably well.

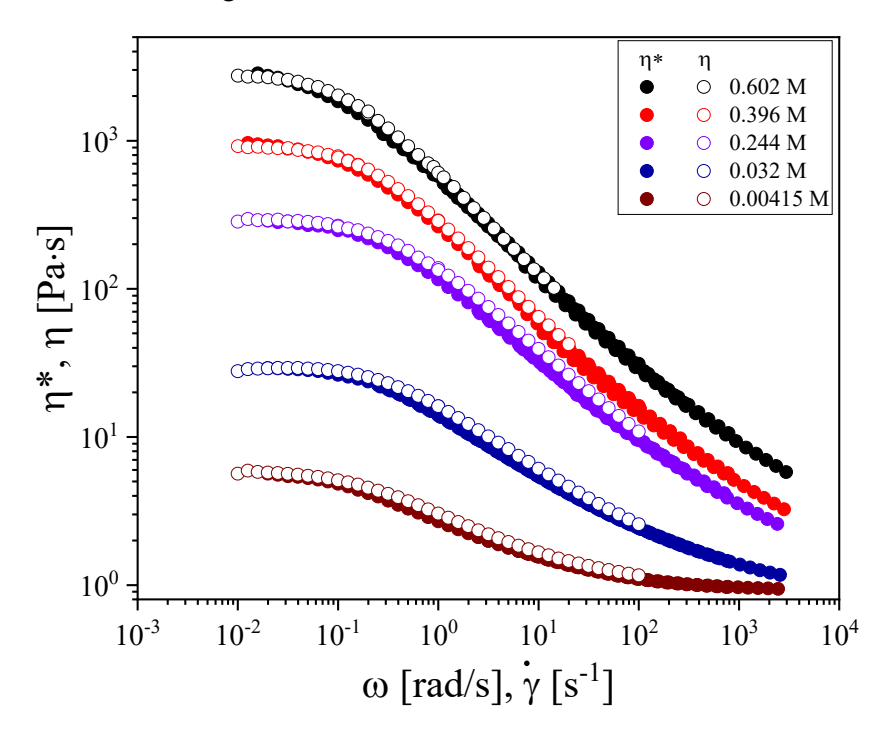


**Figure S3.** Cox-Merz relationship between complex viscosity from the master curves generated from oscillatory experiments (filled symbols) and steady shear viscosity (open symbols) for CsPSS/glycerol solutions of selected concentrations. Higher concentration solutions had steady shear viscosity measurements limited by edge fracture at slightly higher shear rates than reported here. The comparison shows that the polyelectrolyte solutions follow reasonably well the Cox-Merz rule in both unentangled and entangled concentration regimes.